Advances in Engineering Research, volume 204
Proceedings of the 2021 10th International Conference on Applied Science, Engineering and Technology (ICASET 2021)

Parameters Calibration of CT System Based On Geometric Model and Inverse Radon Transform

Huang Hongliang[1], Tang Weiyu[2], Yang Juntao[1], Wang Lidong[1*]

[1]*School of Public Basic and Applied Statistics, Zhuhai College of Jilin University, Zhuhai, Guangdong 519041, China*
[2]*School of Computing, Zhuhai College of Jilin University, Zhuhai, Guangdong 519041, China*

[*]*Corresponding author. Email:wld0707@163.com*

ABSTRACT

CT technology can make use of the penetrability of X-ray to obtain the internal information of the object without damaging the shape and structure of the sample. Therefore, it has a wide range of applications in the fields of industry, non-destructive testing and medical imaging. However, in the installation process of CT system, there are often some problems, such as inaccurate detector spacing, rotation angle and rotation center deviation, resulting in unclear image reconstruction. Thus it is necessary to calibrate the parameters of the installed system with template data, and then image the unknown samples in the process of CT system installation. This paper studies the parameter calibration of CT system. Through the pre-processed data, the analytic geometry model and statistical analysis method are established to calculate the detector interval, 180 rotation angles and rotation center of CT system. In order to verify the accuracy and stability of the parameters, Non-Local Means denoising algorithm (shortly known as NLM denoising algorithm) and Radon inverse transform imaging theorem are introduced. The theoretical image is rebuilt by the absorptivity of the template. The error between the theoretical image and the geometric information of the original template is analyzed, and the fitting is excellent. Two new inhomogeneous media are introduced, and the image is imaged by the parameters obtained from the parameter calibration model and the imaging theorem in this paper. The results are clear and the shadow points are excluded. At the same time, the specific absorptivity of the media is obtained. The calibration model of CT system parameters obtained in this paper, combined with imaging algorithm, can deal with different shapes and irregular conditions. It has great application value in the field of image reconstruction and medicine.

Keywords: *Parameter calibration, Inverse Radon transform, Inverse filtering algorithm, Image reconstruction*

1. INTRODUCTION

CT system can obtain the internal structure information of biological tissue and engineering materials by using the absorption characteristics of the sample to the ray energy without destroying the sample. Due to the X-ray absorption coefficients of different tissue structures are different, the distribution of X-ray absorption coefficients reconstructed by CT can reflect the structural information of the object. At present, CT imaging technology by X-ray has become an important high-resolution, non-invasive and non-invasive detection method.

CT, also known as computerized tomography, can also be used to diagnose the pathological changes of human organs[1]. CT imaging is to convert radiation into visible light. It can convert the visible light into photoelectric signal and convert the photoelectric signal into digital signal. Then the signals are inputted it to the computer and form the image process.

In 1826, Abel, a Norwegian mathematician, who first proposed the concept of tomography when he studied the restoration of cross-section information of axisymmetric objects[2]. In 1917, Austrian mathematician radon

proposed the mathematical method of image reconstruction theory[3]. In 1963, Professor Cormark won the Nobel Prize for further developing an accurate mathematical method for reconstructing images from X-ray projections[4]. Since Hounsfield proposed the tomographic method from 1967 to 1970, the development of CT has been accompanied by the application of mathematical method and computer[5]. In recent years, there are many research methods of CT system parameter calibration. AI Xinchen et al. established the differential equation model of X-ray attenuation according to the Beer Lambert law[6], and established the target programming model based on the least square idea[7] to determine the calibration parameters of the given CT system. Then, the iterative model of CT image reconstruction is built, and the parameters of unknown medium are solved by Richardson algorithm[8]. Finally, the R-L filter function[9] is used to establish the noise reduction model of image reconstruction, and the unknown medium image affected by noise is reconstructed.

Although CT scanning technology is widely used and powerful, errors often incur in the installation to affect the final imaging quality. It is especially important to calibrate the parameters of the installed CT system with the template, and the unknown samples can be imaged accordingly. Based on the data of CUMCM2017, this paper studies the parameter calibration and imaging of two-dimensional CT system. We calibrate the parameters of the installed CT system, that is, calibrate the parameters of the CT system with the help of the sample with known structure (called template), and then image the sample with unknown structure. According to the analytic geometry model (combined with numerical calculation) and statistical analysis method, the analytical solution model is established to obtain the accurate CT system parameters. Non-Local Means denoising algorithm (shortly known as NLM denoising algorithm)[10] is used to process the noise data, and the Inverse Radon Transform is used to reconstruct the image[11] .

2. DATA PREPROCESSING

A calibration template composed of two uniform solid media is placed on a square tray. The geometric information of the template is shown in Figure 1 and the corresponding data file is named " Appendix 1". The value of each point reflects the absorption intensity of the point, which is called "absorptivity". The received information corresponding to the template is named " Appendix 2". According to the known template and its received information, this paper determines the important parameters of the CT system: the position of the rotation center in the square tray, the distance between detector units and the 180 directions of X-ray used by the CT system.

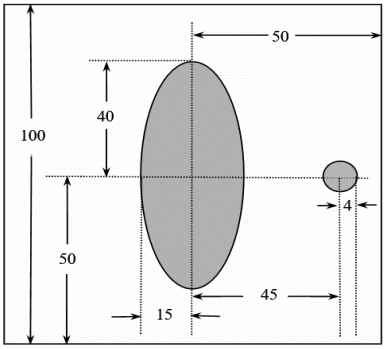

Figure 1 Schematic diagram of formwork (unit: mm)

Based on the analysis of the data, it is assumed that the first light is the first light on the left. First, the data file (256×256) in Appendix 1 and the data file (180×512) in Appendix 2 are processed by Excel. Then, the two-color scale and three-color scale in Excel table are used to distinguish different sizes of data in the table, and Figure 2 is obtained.

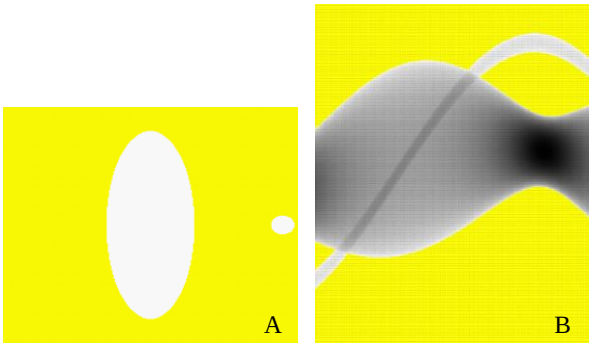

Figure 2 Color scale processing chart

(A: data processing in Appendix 1;
B: data processing in Appendix 2)

In Figure 2. A, the value of each point in the square tray reflects the absorption intensity of the point. Using Excel two-color scale, the maximum value is white and the minimum value is yellow, so Figure 2. A is obtained. In

Figure 2. B, column 180 represents 180 directions, and row 512 represents the received information of the template after a total of 512 lights pass through the whole square tray in each direction, in which yellow represents the value of 0, that is, the absorptivity and received information are 0. Using Excel three color scale, set the minimum value as yellow, the percentage of 0-50 as white, and the maximum value as black to get Figure 2. B. Next, the special situation of X-ray in 180 directions in Appendix 2 is further analyzed, and the geometric model of parameter calibration is established.

3. GEOMETRIC MODEL OF PARAMETER CALIBRATION

3.1. Two methods of determining detector interval calculation

Since the medium is uniform, we assume that the medium is ellipse and circle, and take the ellipse center as the original center to establish a rectangular coordinate system on the square tray, as shown in Figure 3.

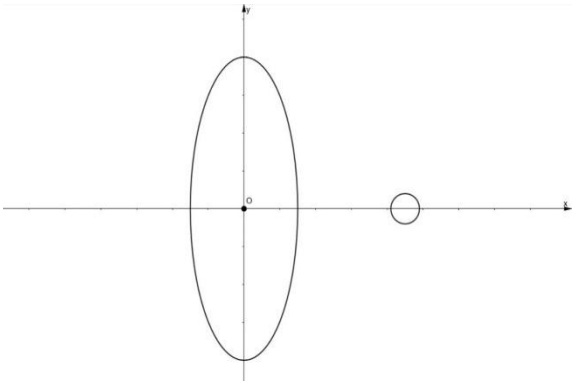

Figure 3 Establishment diagram of coordinate axis

First, set the detector spacing distance as d. In Cartesian coordinates, the elliptic equation is:

$$\left(\frac{x}{15}\right)^2+\left(\frac{y}{40}\right)^2=1 \quad (1)$$

And the circular equation is:

$$(x-45)^2+y^2=16 \quad (2)$$

By calculation, the major axis of the ellipse is 80mm, the minor axis is 30mm, and the radius of the circle is 4mm. Through the analysis of color scale accessories, it is found that there are 108-109 ellipses with the least radiation (that is, the X-ray is parallel to the major axis of the ellipse and perpendicular to the minor axis of the ellipse). Supposing the minor axis of the ellipse is l_1, we gain the following inequality.

$$108d < l_1 < 109d \quad (3)$$

Through the solution, we can get the following inequality.

$$0.2752 < d < 0.2778 \quad (4)$$

Through the analysis of color scale accessories, it is found that there are 289 ellipses that are irradiated by X-ray (that is, X-ray is parallel to the minor axis of ellipse and perpendicular to the major axis of ellipse). The major axis of the ellipse is l_2, get the inequality.

$$288d < l_2 < 290d \quad (5)$$

Through the solution, we can get the following inequality.

$$0.2759 < d < 0.2778 \quad (6)$$

Through the analysis of color scale accessories, it is found that there are 28-19 circles in 180 directions irradiated by X-ray. We supposed the diameter of the circle is l_3, so we can get the following inequality.

$$28d < l_3 < 29d \quad (7)$$

Through the solution, we can obtain the inequality.

$$0.2759 < d < 0.2857 \quad (8)$$

The detector distance d was calculated by combining l_1, l_2, l_3. the inequality is as follows.

$$0.2759 < d < 0.2778 \quad (9)$$

Method 1: Calculation of detector separation distance based on Statistical Analysis

By analyzing the data and color scale image in Appendix 2, assuming that the X-ray is a straight line. For the ellipse and circle in the tray, M371-M373 column in Excel data sheet is the internal common tangent with a positive slope, and DE111 column is the internal common tangent with a negative slope. It is ignored because the external common tangent of ellipse and circle is unstable and the error is large. These cases are ignored because there are some cases in M-DE column in which elliptical medium and circular medium receive the same beam of light. The receiving information of X-ray in A-M and DE-FX

columns after passing through the spherical medium on the right side of the square tray is extracted, with a total of 1190 data. Each data is filtered, and the maximum value is MAX=14.1796. The chord length obtained by the X-ray of this data passing through the circle is closest to the diameter of the circle, which is 8mm in diameter. Assuming that the received inform ation of a circle is proportional to the length of the X-ray passing through the circular medium, then their ratio relationship is approximately $k = \frac{14.1796}{8} = 1.7725$.

It is assumed that the two-dimensional template medium is uniform. Let $\Delta l = ky_i$. Where y_i is the energy absorbed per unit length (gain after X-ray attenuation) and is the unit length.

Geometric analysis of any two rays passing through a circle is performed, as shown in Figure 4.

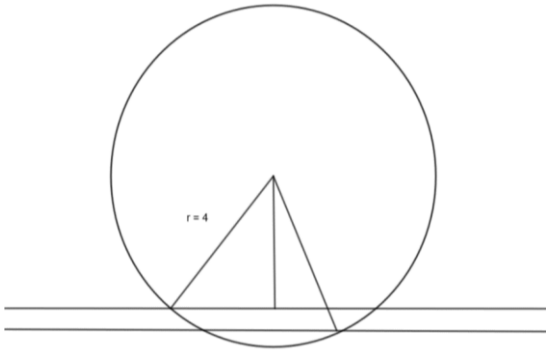

Figure 4 Geometric analysis diagram of circle

Get the mathematical model, as shown in Equation(10).

$$y_i = \sqrt{r^2 - \left(\sqrt{r^2 - \frac{y_{i+1}^2}{4}} - d\right)^2} \tag{10}$$

Where i is the number of 512 beams and d is the distance between detectors. Continue to work together to get Equation(11).

$$kx_i = \sqrt{k^2r^2 - \left(\sqrt{k^2r^2 - \frac{k^2x_{i+1}^2}{4}} - kd\right)^2} \tag{11}$$

Since k is known and the radius of the circle $r = 4mm$, the x_i information in columns A-M and DE-FX is substituted into the mathematical model, and the received information of each circle with different data has 28-29 groups of data. Taking 14 groups of data, we get the vertical energy of the 14 X-rays passing through the circle from the center of the circle and calculate the energy difference of each adjacent X-ray in Excel. Then we calculate the average value of the energy difference. Finally, we divide the data by k to get d . The average value of all data is calculated, so we get the optimal interval $d = 0.2768mm$, which satisfies the range of d .

Method 2: Mathematical model of detector spacing calculation based on Analytic Geometry.

By the first method and through the geometric analysis of the circle, we select any two internal lines in the same direction to analyze, and get the mathematical model between the two adjacent lines as shown in Equation(14).

$$\sqrt{r^2 - \frac{x_i^2}{2^2}} - \sqrt{r^2 - \frac{x_{i+1}^2}{2^2}} = d \tag{12}$$

After combining with Δl and removing the root sign, we get the following Equation(13).

$$\left(32 - \frac{x_t^2 + x_{t+1}^2}{4k^2} - d^2\right)^2 = 4\left(16 - \frac{x_t^2}{4k^2}\right)\left(16 - \frac{x_{t+1}^2}{4k^2}\right) \tag{13}$$

The equations are established by the data in the appendix. After following, we gain Equation(14) and Equation(15) as following.

$$\begin{cases} \left(32 - \frac{x_t^2 + x_{t+1}^2}{4k^2} - d^2\right)^2 = 4\left(16 - \frac{x_t^2}{4k^2}\right)\left(16 - \frac{x_{t+1}^2}{4k^2}\right) & (14) \\ \left(32 - \frac{x_{t+1}^2 + x_{t+2}^2}{4k^2} - d^2\right)^2 = 4\left(16 - \frac{x_{t+1}^2}{4k^2}\right)\left(16 - \frac{x_{t+2}^2}{4k^2}\right) & (15) \end{cases}$$

The relationship between k and d is obtained by MATLAB programming, as shown in Equation(16) and Equation(17).

$$k = \frac{1}{2}\sqrt{\frac{(x_t - 2x_{t+1} + x_{t+2})(x_t + 2x_{t+1} + x_{t+2})(x_t + 2x_{t+1} - x_{t+2})(-x_t + 2x_{t+1} + x_{t+2})}{128\,(x_t^2 - 2x_{t+1}^2 + x_{t+2}^2)}} \tag{16}$$

$$d = \frac{8\,(x_t^2 - 2x_{t+1}^2 + x_{t+2}^2)}{\sqrt{(-x_t + 2x_{t+1} - x_{t+2})(x_t + 2x_{t+1} + x_{t+2})(x_t + 2x_{t+1} + x_{t+2})(x_t + 2x_{t+1} - x_{t+2})(-x_t + 2x_{t+1} + x_{t+2})}} \tag{17}$$

All the k and d values obtained by x_i are solved by MATLAB programming. The average value of all k and d is obtained to get optimal $k = 1.7725$, $d = 0.2768mm$.

The results of the two methods are analyzed:

Method 1 and method 2 are based on a large number of processing and analysis of the data in Appendix 1 and Appendix 2 and the interval range obtained after analysis. The difference is that method 1 is the result obtained by special X-ray. The second method is to establish the equations of k and d, solve k and d for all the extracted data, and get the best answer.

3.2. Determination of rotation angle based on elliptic chord length and Veda theorem

In the established rectangular coordinate system, the width of X-ray is ignored. Each angle of 512 rays is regarded as 512 linear equations with the same slope (each slope error is small) but different intersections on the y axis. The X-ray receiving information that only passes the elliptic equation but not the circular equation is screened out in Appendix 2, because the proportion coefficient of receiving information and ray length is $k = 1.7725$. We get the relation between the received information and the chord length of the ellipse as $t = \frac{J}{k}$. Therefore, through the calculation formula of chord length of ellipse and Weida's theorem, three equations about the slope m and the intersection $b1$ and $b2$ of two adjacent lines on y axis can be obtained. This is shown below.

$$\begin{cases} t_{jn}^2 = [\dfrac{4\times 15^2 m_j^2 b_{jn}^2}{\left(40^2 + 15^2 m_j^2\right)^2} - \dfrac{4\times 15^2 (b_{jn}^2 - 40^2)}{40^2 + 15^2 m_j^2}](1 + m_j^2) & (18) \\ t_{(j+1)n}^2 = [\dfrac{4\times 15^2 m_j^2 b_{(j+1)n}^2}{\left(40^2 + 15^2 m_j^2\right)^2} - \dfrac{4\times 15^2 (b_{(j+1)n}^2 - 40^2)}{40^2 + 15^2 m_j^2}](1 + m_j^2) & (19) \\ d^2(1 + m_j^2) = \left(b_{jn}^2 + b_{(j+1)n}^2\right)^2 & (20) \\ m_j = m_{j+1} & (21) \end{cases}$$

Where m_j is the slope of the $j-th$ ray and b_{jn} is the intercept of the $j-th$ ray in the $n-th$ direction.

Because assuming that the slopes of 512 rays are the same, the slopes of one ray in each direction can be solved. We can get 180 groups of m by solving the equation with MATLAB. Because m value has positive and negative values, through the analysis of the geometric information of the square tray, it can be concluded that the slope of the first ray in Appendix 2 must be negative to meet the arrangement of the received information in column A. Therefore, all slopes m are listed, and the inclination angle of X-ray is obtained by inverse trigonometric function, as shown in **Table 1**.

Table 1 180 Tilt angles of X-ray

-60.3538	-59.0000	-58.4448	-57.3554	-56.3230	-55.3539	-54.3538	-53.3539	-52.3537	-51.3539
-50.3539	-49.3537	-48.3534	-47.3538	-46.3539	-45.2037	-44.3537	-43.3537	-42.3539	-41.3537
-40.3540	-39.3533	-38.3532	-37.3541	-36.3531	-35.3529	-34.3539	-33.3540	-32.3541	-31.3542
-30.3540	-29.4551	-28.3540	-27.3536	-26.3537	-25.3533	-24.3538	-23.3537	-22.3532	-21.3534
-20.3539	-19.3528	-18.3554	-17.3533	-16.3529	-15.3546	-14.3540	-13.3539	-12.3535	-11.3544
-10.3528	-9.3541	-8.3544	-7.3529	-6.3523	-5.3490	-4.3505	-3.3520	-2.3614	-1.3588
-0.2825	0.6466	1.6651	2.6515	3.6428	4.6479	5.6480	6.6446	7.6460	8.6485
9.6465	10.6457	11.6467	12.6459	13.6483	14.6463	15.6467	16.6474	17.6454	18.6454
19.6455	20.6460	21.6458	22.6463	23.6467	24.6464	25.6466	26.6459	27.4436	28.6466
29.6468	30.6467	31.6460	32.6463	33.6469	34.6459	35.6467	36.6464	37.6461	38.6464
39.6464	40.6463	41.7461	42.6465	43.6460	44.6462	45.6467	46.6462	47.6462	48.6463
49.6463	50.6461	51.6465	52.6462	53.6465	54.6462	55.6462	56.6464	57.6462	58.6463
59.6464	60.6463	61.6462	62.6464	63.6462	64.6461	65.6464	66.6464	67.6464	68.6464
69.6462	70.6463	71.6462	72.6462	73.6463	74.6464	75.6464	76.6463	77.6462	78.6462
79.6462	80.6464	81.6462	82.6462	83.6462	84.6462	85.6461	86.6461	87.6462	88.6461
89.6464	-89.3529	-88.3541	-87.3537	-86.3540	-85.3539	-84.3538	-83.3538	-82.3538	-81.3538
-80.3538	-79.3537	-78.3537	-77.3539	-76.3538	-75.3538	-74.3536	-73.3538	-72.3538	-71.3538
-70.3538	-69.3539	-68.3538	-67.3538	-66.3539	-65.3537	-64.3539	-63.3537	-62.3537	-61.3642

3.3. Determination of rotation center based on geometric model of angular bisector

We extract the data of 189 rows in A column, 189 rows in B column and 189 rows in C column of Excel, and calculate t . Then we use the equations established above to find the M and b values of the three cells. Because it is the first, second and third direction, through the change trend of the data in Appendix 2, the straight line of b value with positive slope and greater than 0 is eliminated. $L1$, $L2$ and $L3$ are obtained.

$L1$: $y = -1.756807246x - 47.77288099$ (22)

$L2$: $y = -1.664074971x - 45.4181973$ (23)

$L3$: $y = -1.62814129x - 44.51095923$ (24)

Three straight line equations through the ellipse, and then find the angle bisector of two adjacent lines, a total of four. However, the angle bisector with larger angle between two straight lines will make the center of rotation better, hence the equation of two angle bisectors is obtained. Finally, the intersection point, the center of rotation, is obtained. Three equations are inputted through the Geometer's Sketchpad to obtain the equations of two bisectors. Equation(25) and Equation(26) are the solutions.

Bisectors of angles $L1$ and $L2$:

$$y = 0.5849648129764x + 11.6900457307071 \quad (25)$$

Bisectors of angles L2 and $L3$:

$$y = 0.56075463724188x + 11.9347180156909 \quad (26)$$

The intersection point is obtained, and the center of rotation is $(-10.8350, 5.3519)$.

4. IMAGE RECONSTRUCTION BASED ON INVERSE RADON TRANSFORM

4.1. NLM denoising algorithm

Image reconstruction algorithm will cause artifacts in the image. At the same time, due to the noise in the data, the image quality is poor and there are shadows. In this paper, NLM is used to process the image. NLM algorithm[11] is one of the most effective algorithms in the field of image denoising, with high efficiency and simple implementation. The principle of the algorithm is to average the gray values of the pixels in a neighborhood window. The larger the weight is, the similar the pixels are.

$$NLM = \sum_{k \in N_i} w(i,k) x_k \tag{27}$$

Where

$$w(i,k) = \frac{e^{-\left\| x_{vi} - x_{vk} \right\|^2 / h^2}}{\sum_{k \in N_i} e^{-\left\| x_{vi} - x_{vk} \right\|^2 / h^2}} \tag{28}$$

4.2. Inverse filtering algorithm based on inverse Radon transform

When X-ray passes through the medium of uniform material, the attenuation rate of its intensity is directly proportional to the intensity itself as follows Equation(29).

$$\frac{dI}{dl} = -\mu l \tag{29}$$

Where I is the intensity of the ray, l is the thickness of the material in the direction of the ray, and μ is the attenuation coefficient of the material to the radiation[12], thus Equation(30) can be obtained.

$$I = I_0 e^{-\mu l} \tag{30}$$

where I_0 is the incident intensity of X-ray. When the energy of X-ray is constant, the attenuation coefficient μ varies with the material through which the X-ray passes.

When the X-ray passes through a non-uniform medium composed of materials with different coefficients, such as a section inside the medium. μ is the function $\mu(x, y)$ of a plane coordinate x, y. When the X-ray passes along the internal straight line L of the x-y plane, Equation(31) is obtained.

$$I = I_0 e^{-\int_L \mu(x,y) dl} \tag{31}$$

Where $\int_L \mu(x,y) dl$ is the line integral $\mu(x, y)$ along L. Taking logarithms on both sides at the same time, we get Equation(32).

$$\int_L \mu(x,y) dl = \ln \frac{I_0}{I} \tag{32}$$

If the integrand function is determined according to Equation (32), the attenuation coefficient of X-ray can be calculated according to the cross sections of human body and other media. At the same time, we can get the size, shape, density and other image information of human organs and media, namely image reconstruction.

The expression of the inverse transform of radon integral change is given in reference[12].

$$P_f(L) = \int_L f(x,y) dl \tag{33}$$

Equation(33) is that radon transform takes any point Q (x, y) as a point and takes the line integral $\int_L f(x,y) dl$ of a straight line d away from Q point. Taking the average value of all $\int_L f(x,y) dl$ get Equation(34).

$$f(Q) = -\frac{1}{\pi} \int_0^\infty \frac{dF_Q(d)}{d} \tag{34}$$

Through Equation(34), the rotation center of the square tray, the detector spacing, and the rotation angle, we can determine the position of the medium, the geometry and the specified absorptivity

5. ACCURACY AND STABILITY ANALYSIS

The rectangular coordinate system is re-established so that the coordinates of the rotation center are all positive numbers, and get the rotation center $(10.8350, 5.3519)$, as shown in Figure 5.

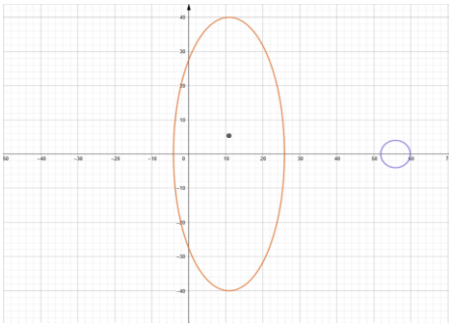

Figure 5 The position of the redefined coordinate system

Because the size of the geometric information table and the absorptivity table are different, the ratio of the two tables is $U = \frac{100}{256} = 0.3906$. Through the rotation center, the detector spacing and 180 rotation angles, 512 X-ray beams in 180 directions are solved by line integration. Using the method of inverse Radon transform[13][14] we can realize the imaging by inverse Radon transform method by using the iRadon function in MATLAB. Combined with the X-ray absorptivity information table of known media, the imaging effect is shown in Figure 6.

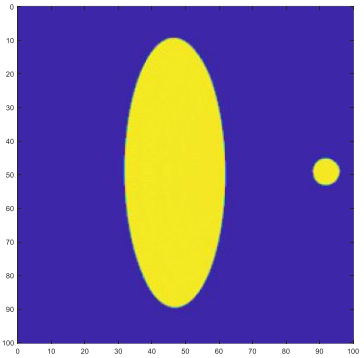

Figure 6 Matlab imaging of Appendix 2

First of all, we need a standard to measure the accuracy and stability of CT system parameter calibration. For the stability, the parameters of CT system are used to analyse the error of the parameters obtained by the model, and to analyse whether the changes of the calibrated parameters are stable. For accuracy, the template is fitted by the calibrated CT system parameters after the model is solved. We calculate the absorption intensity of the template, and then compare it with the actual template to see whether it is accurate fitting.

The accuracy and stability of the calibration parameters of CT system are tested. Firstly, the stability of the CT system is analyzed. Then 180 slopes in 180 directions are obtained through the model. Next, 180 rotation angles can be obtained by the slope. The average value of the difference can be obtained by 179 difference values of two adjacent rotation angles. Finally, the error of rotation angle is obtained by the difference between two adjacent data. We use SPSS to draw a line chart of the error value, as shown in Figure 7.

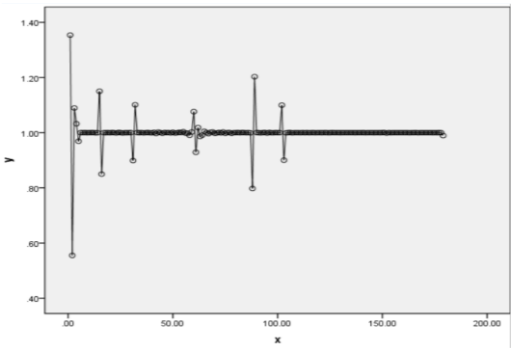

Figure 7 Error analysis chart of rotation angle by SPSS

It can be clearly seen from Figure 8 that the error of rotation angle is small, no more than 0.4, and it can be seen from the chart that the error will be corrected after the error is generated. The influence of the error on the mean value is reduced by a great extent, and tends to be flat later. This shows that the stability of CT system parameter calibration is high and the parameters are reasonable.

For the accuracy analysis of parameter calibration, through the mathematical model of inverse filtering, the iRadon function in MATLAB is used for programming. We import the received information of the known medium in Appendix 2 into MATLAB code to get the geometric information and the absorptivity table of the known medium, and use Appendix 1 and the absorptivity table to make a difference between the cells to get the difference. At the same time, the color scale is processed, as shown in Figure 8.

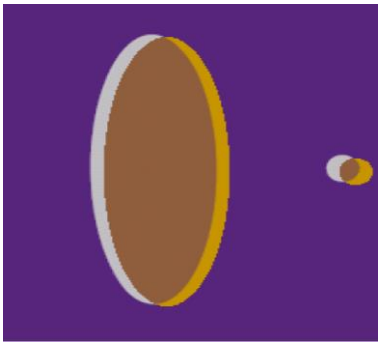

Figure 8 Accuracy analysis chart of parameter calibration

The purple value is 0, the silver value is negative, the orange value is 1, and the brown value is not a positive number. We can see that the fitting degree of elliptic medium is higher, which indicates that the accuracy of calibrated parameters is reasonable, but the fitting degree

of circular medium can continue to be improved. It indicates that the accuracy can continue to be improved.

6. IMAGING EXPERIMENT AND ABSORPTIVITY RESEARCH

In order to verify the imaging effect of calibration parameters, two kinds of irregular media are selected for imaging. One is the superposition of multiple regular media to get new media, the other is irregular media. By importing data from different media (i.e. receiving information of media), the position and geometry of media are solved, and 256×256 absorptivity information is obtained. We solve the same information for different media. First, the absorptivity tables of the two media are processed by color scale, and Figure 9 is obtained.

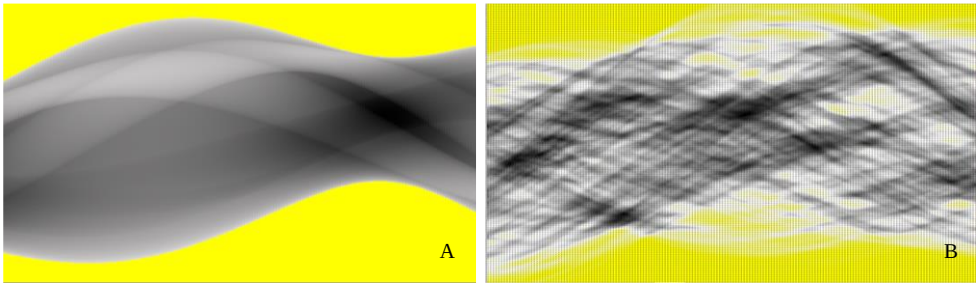

Figure 9 Color scale processing diagram (A: color scale processing for overlapping media; B: color scale processing for irregular shaped media)

Then, iRadon function of MATLAB is used to solve the problem. At the same time, we import the data of the absorptivity of the two media. We get the geometric information of the media and the position of the media in the square tray, and get the 256×256 absorptivity table and imaging effect, as shown in Figure 10.

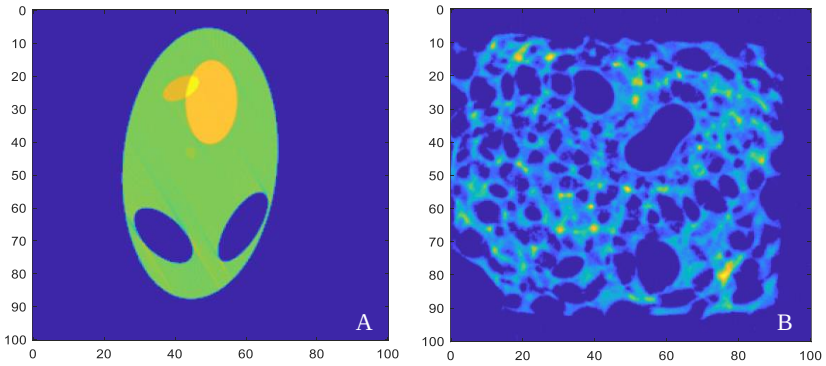

Figure 10 Experimental image (A: Geometry of overlapping media; B: Geometry of irregular media)

Through calculating the data of absorptivity, we compare the real value with the theoretical value, and analyse the results combined with the image reconstruction algorithm in this paper. Draw a table, as shown in Table 2.

Table 2 Result analysis

	Media	Clear or not	Absorptivity of each point obtained or not
Object1	Overlapping media	clear	√
Object2	Irregular media	clear	√

The experimental results show that the geometric model established in this paper can effectively and accurately calculate the parameters of CT system. Combined with NLM denoising algorithm and radon inverse transform image reconstruction model, it can clearly image regular material, overlapping material, irregular material and other media, and calculate the X-ray absorptivity of each point. It is widely used in the field of nondestructive testing and

medical imaging[15] (such as bone detection vascular imaging, cardiac imaging, breast imaging, dental imaging, etc.).

7. CONCLUSION

In this paper, the important parameters of CT system (detector spacing, rotation angle and rotation center) are calibrated based on analytic geometry model and statistical analysis method. The imaging experiments are carried out by NLM denoising algorithm and radon inverse transform model. The stability and accuracy of the parameters are verified by error analysis. Finally, the inhomogeneous medium is introduced for imaging to obtain clear and shadow free images. The experimental results show that the parameters of the geometric model are reasonable, and can deal with the imaging of different shapes of objects. It has practical significance and application value in the field of image reconstruction and medicine.

ACKNOWLEDGMENT

This work was supported by 2020 National Entrepreneurship Training Program for College Students (202013684002).

REFERENCES

[1] Kak, Avinash, C, et al. Principles of Computerized Tomographic Imaging[J]. Medical Physics, 2002.

[2] Hsieh, J. A generalized helical reconstruction algorithm for multislice CT[J]. Radiology, 2000, 217P, 565.

[3] Radon J . Uber die bestimmung von funktionen durch ihre integralwerter langs gewissen manning faltigkeiten.[J]. Ber Saechs Akad Wiss Leipzig Math-Phys, 1917, 69.

[4] Cormack A M . Representation of a Function by Its Line Integrals, with Some Radiological Applications[J]. Journal of Applied Physics, 1963, 34(9):2722-2727.

[5] Hounsfield G N. A method of and apparatus for examination of a body by radiation such as X-or gamma-radiation[J]. British Patent No. 1,283,915, 1972.

[6] Xin-Chen AI , Yong-Kang L , Lu Z . The Parameter Calibration for a CT System and CT Imaging[J]. Journal of Nantong Vocational University, 2018. (In Chinese)

[7] Long K , Zuo Z , Zuberi R H . Study on parameters for topological variables field interpolated by moving least square approximation[J]. Acta Mechanica Solida Sinica, 2009, 22(002):180-188.

[8] Liu Wei-hao,Mei Lin,Cai Xuan.Regularized image restoration algorithm on sparse gradient prior model[J]. Journal of Image and Graphics, 2012, 17(12):1485-1491. (In Chinese)

[9] Shi BY,Wang C, Chen SH, et al. A novel method of CT reconstruction filter function design[J]. CT Theory andApplications, 2010, 19(4): 35-43. (In Chinese)

[10] CHEN Xing,SONG Zhi-yang,ZHOU Ming-quan,WU Zhong-ke,WANG Xing-ce. An improved non-local mean filter filtering algorithm facing the cerebrovascular segmentation[J]. Chinese Optics, 2014, 7(4): 572-580. (In Chinese)

[11] Han Yu, Li Lei, Yan Bin, Xi Xiao-Qi, Hu Guo-En. A half-covered helical cone-beam reconstruction algorithm based on the Radon inversion transformation. Acta Physica Sinica, 2015, 64(5): 058704. (In Chinese)

[12] Jiang Q, Xie J X, Ye J. Mathematical model[J]. The Press of High Education, Beijing, 2003: 227-228. (In Chinese)

[13] Zhang P, Zhang Z. Research and comparison on several CT reconstruction algorithms[J]. Computerized Tomography Theory and Applications, 2001, 10(4): 4-10. (In Chinese)

[14] He Yongjun. CT image reconstruction with fast back projection and transformation [D]. Beijing

University of Posts and telecommunications, 1993. (In Chinese)

[15] Lu Yanbin. X-ray CT imaging and multimodality imaging [D]. Peking University, 2012. (In Chinese)

[16] P. Xu, Research and application of near-infrared spectroscopy in rapid detection of water pollution, Desalination and Water Treatment, 122(2018)1-4.

[17] P. Xu; N. Na; S. Gao; C. Geng, Determination of sodium alginate in algae by near-infrared spectroscopy, Desalination and Water Treatment, 168(2019)117-122.

[18] P. Xu, N. Na, Study on Antibacterial Properties of Cellulose Acetate Seawater Desalination Reverse-Osmosis Membrane with Graphene Oxide, Journal of Coastal Research, 105(2020)246-251.